AL/CF-TR-1994-0033

AD-A284 849

‖ A R M S T R O N G   L A B O R A T O R Y

ECHO IMAGING TECHNIQUES DETERMINE THE SIZE OF INTRAVASCULAR BUBBLES IN DECOMPRESSION SICKNESS

Robert M. Olson

Rothe Development, Incorporated
4614 Sinclair Road
San Antonio, TX 78222

CREW SYSTEMS DIRECTORATE
CREW TECHNOLOGY DIVISION
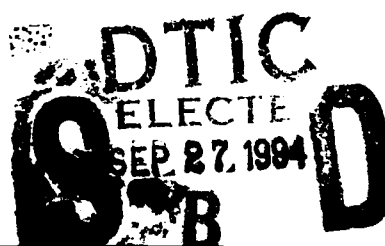2504 D Drive, Suite 1
Brooks Air Force Base, TX 78235-5104

July 1994

Final Technical Report for Period March 1992 – May 1993

94-30753

DTIC
ELECTE
SEP 27 1994
B

94 9 26 086

AIR FORCE MATERIEL COMMAND
BROOKS AIR FORCE BASE, TEXAS

NOTICES

When Government drawings, specifications, or other data are used for any purpose other than in connection with a definitely Government-related procurement, the United States Government incurs no responsibility or any obligation whatsoever. The fact that the Government may have formulated or in any way supplied the said drawings, specifications, or other data, is not to be regarded by implication, or otherwise in any manner construed, as licensing the holder, or any other person or corporation; or as conveying any rights or permission to manufacture, use, or sell any patented invention that may in any way be related thereto.

The voluntary, fully informed consent of the subjects used in this research was obtained as required by AFR 169-3.

The Office of Public Affairs has reviewed this report, and it is releasable to the National Technical Information Service, where it will be available to the general public, including foreign nationals.
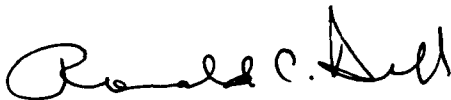
This report has been reviewed and is approved for publication.

ANDREW A. PILMANIS, Ph.D.
Project Scientist

F. WESLEY BAUMGARDNER, Ph.D.
Chief, Systems Research Branch

RONALD C. HILL, Colonel, USAF, BSC
Chief, Crew Technology Division

REPORT DOCUMENTATION PAGE

1. AGENCY USE ONLY (Leave blank)	2. REPORT DATE July 1994	3. REPORT TYPE AND DATES COVERED Final – March 1992 – May 1993

4. TITLE AND SUBTITLE
Echo Imaging Techniques Determine the Size of Intravascular Bubbles in Decompression Sickness

6. AUTHOR(S)
Robert M. Olson

5. FUNDING NUMBERS
C – F33615-89-D-0604
PE – 62202F
PR – 7930
TA – 18
WU – Y2

7. PERFORMING ORGANIZATION NAME(S) AND ADDRESS(ES)
Rothe Development, Incorporated
4614 Sinclair Road
San Antonio, TX 78222

8. PERFORMING ORGANIZATION REPORT NUMBER

9. SPONSORING/MONITORING AGENCY NAMES(S) AND ADDRESS(ES)
Armstrong Laboratory (AFMC)
Crew Systems Directorate
Crew Technology Division
2504 D Drive, Suite 1
Brooks Air Force Base, TX 78235-5104

10. SPONSORING/MONITORING AGENCY REPORT NUMBER
AL/CF-TR-1994-0033

11. SUPPLEMENTARY NOTES

Armstrong Laboratory Technical Monitor: Dr. Andrew A. Pilmanis, (210) 536-3545.

12a. DISTRIBUTION/AVAILABILITY STATEMENT

Approved for public release; distribution is unlimited.

12b. DISTRIBUTION CODE

13. ABSTRACT (Maximum 200 words)

The size of altitude induced intravenous bubbles was determined. These bubbles, referred to as venous gas emboli (VGE), are thought to be a major factor in the onset and severity of decompression sickness (DCS). Ten volunteer subjects were monitored for altitude induced VGE in the inferior vena cava (IVC) with a HP Sonos 1000 echo imaging system. Bubble size was determined indirectly and by in-vitro sizing methods because ultrasonic images do not necessarily represent true VGE size. Stratification of bubbles of known size in a water filled mechanical analog of the IVC determined the upper size limit, which was 300 μM in these experiments; bubbles larger than 300 μM roll along the top of the vessel. The lower size limit was the size of the smallest bubbles which the Sonos 1000 could image, determined indirectly by in-vitro microbubble flotation rates and survival times measured ultrasonically and calibrated microscopically. The diameter of the smallest VGE which echo imaging systems can detect in the IVC was found to be 30-40 μM. Used in this determination was the fact that these microbubbles are too small to float; they survive less than a minute. In conclusion, the size of the ultrasonically detected VGE in the interior of the IVC of decompressed subjects can be measured; for subjects at 29,500 ft. bubble size varied from 30-300 μM.

DTIC QUALITY

14. SUBJECT TERMS
Bubble size
Decompression sickness
Echo imaging

15. NUMBER OF PAGES
36

16. PRICE CODE

17. SECURITY CLASSIFICATION OF REPORT Unclassified	18. SECURITY CLASSIFICATION OF THIS PAGE Unclassified	19. SECURITY CLASSIFICATION OF ABSTRACT Unclassified	20. LIMITATION OF ABSTRACT UL

CONTENTS

Figures

Figures (Continued)

ACKNOWLEDGMENTS

Accession For	
NTIS GRA&I	☑
DTIC TAB	☐
Unannounced	☐
Justification	

By	
Distribution/	
Availability Codes	

Dist	Avail and/or Special
A-1	

ECHO IMAGING TECHNIQUES DETERMINE THE SIZE OF INTRAVASCULAR BUBBLES IN DECOMPRESSION SICKNESS

INTRODUCTION

Separation of supersaturated gas in the form of bubbles is associated with decompression sickness (DCS). These bubbles are thought to cause DCS symptoms by disrupting tissue integrity, by direct nerve stimulation, or by the ischemia produced by vascular occlusion (3). Although the bubbles have been detected ultrasonically in the venous system for many years (5,7), it has not been possible to determine their size. The role of intravascular bubbles in DCS will be better understood when bubble size is known. For example, bubble size will help define the origin and destiny of intravenous bubbles (venous gas emboli, VGE). VGE larger than 15 µM are too big to originate from capillaries and will have difficulty traversing the pulmonary circulation (3). As another example, consider "silent" or asymptomatic bubbles. It has been demonstrated that when subjects are exposed to low altitude, few, if any, develop DCS. However, VGE are often detected (2) in these subjects. Therefore, it follows that VGE must reach a threshold size before symptomatic DCS develops. If this assumption holds true, the bubble size at which symptoms occur in decompressed subjects can be used as an endpoint in predicting DCS risk . In order to prove this concept, however, actual bubble size measurements in decompressed subjects may be necessary. Similarly, computer modeling of DCS risk prediction requires accurate bubble growth equations (4). Such mathematical algorithms must be verified with in-vivo measurements (8).

There are a few articles in the literature describing possible techniques to measure bubble size, but none has been successfully applied to decompressed human subjects (1,6). A number of problems are encountered not only in the instrumentation and techniques, but in some basic assumptions. For example, there may not be just one bubble size, but a range of sizes. Bubbles in different sites may have different size ranges. Also, any given bubble may be growing and not have a static size.

Ultrasonic echo imaging instruments are now available which can display bubble images in decompressed subjects. However, the size of these images, shown on a television screen, does not correlate well with the actual bubble size. The purpose of this study was, first, to show that echo imaging systems can be used to estimate the size of circulating VGE, and, second, to document the size range of ultrasonically detected VGE associated with DCS at 29,500 ft. These size measurements would then be available to verify computed sizes and improve the understanding of the underlying physiology of DCS.

METHODS

Instrumentation

The echo imaging system (H.P. Sonos 1000) used in this study is shown in Figures 1 and 2. Figure 2 shows the transducer with an illustration of the emitted ultrasonic beam which is fan shaped and occupies a single plane. Structures in the path of this beam appear on the monitor of the instrument, as shown in Figure 3. This figure shows a sector scan made by the Sonos 1000 when the probe was placed on a subject's abdomen just below (caudal to) the sternum. The plane of the ultrasonic beam emitted from the probe, as shown in Figure 2, passed through the liver and part of the heart. The IVC which passes through the liver was also in the beam. Figure 3 shows the resulting triangular sector scan, where the apex at the top images structures nearest to the probe. Note a line of dots extending from the apex to the bottom of the sector. These are depth markers; the distance between two adjacent dots represent 1 cm of tissue depth. The inferior vena cava (IVC) is shown in the bottom of this figure as a horizontal 1-cm thick black band through the liver, about 10 cm from the probe, going to the heart.

The Sonos 1000 is shown at the top of Figure 1. The monitor screen which displays images of VGE in various vessels can be seen near the top of the instrument. The bottom of Figure 1 shows the vertical control panel which is just to the right of the screen and the "keyboard" which is immediately below the screen. Two knobs which are especially important in bubble sizing are located near the middle of the vertical control panel, one labeled "transmit" and the other labeled "compress". If either of these controls is set too low, small bubbles may not be imaged. If the compress knob is set too high, "snow" (electronic noise), which may be confused with bubbles, appears. If the transmit knob is set too high, structures tend to run together.

Subject Protocol

The Sonos 1000 was used to display venous gas emboli in human subjects. Ten healthy male subjects, age 21 to 35, were monitored with the Sonos 1000 while they participated in an ongoing high-altitude study. The subjects breathed 100% oxygen 1 h before exposure and for the duration of the flight, using a neck-seal respirator (Intertechnique Corporation, France) designed for comfort and freedom from gas leaks. The system was slightly pressurized (2 in. H_2O) so that any leaks would be outboard. The subjects were then taken to a simulated altitude of 29,500 ft. At altitude, the subjects performed light lower body exercise on a weight machine for 4 out of every 20 min. Then they rested for 5 min after which they were monitored for VGE going through the heart following sequential joint flexion. A technician inside the
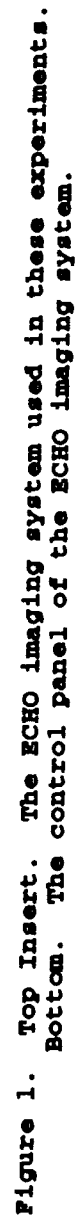
Figure 1. Top Insert. The ECHO imaging system used in these experiments. Bottom. The control panel of the ECHO imaging system.
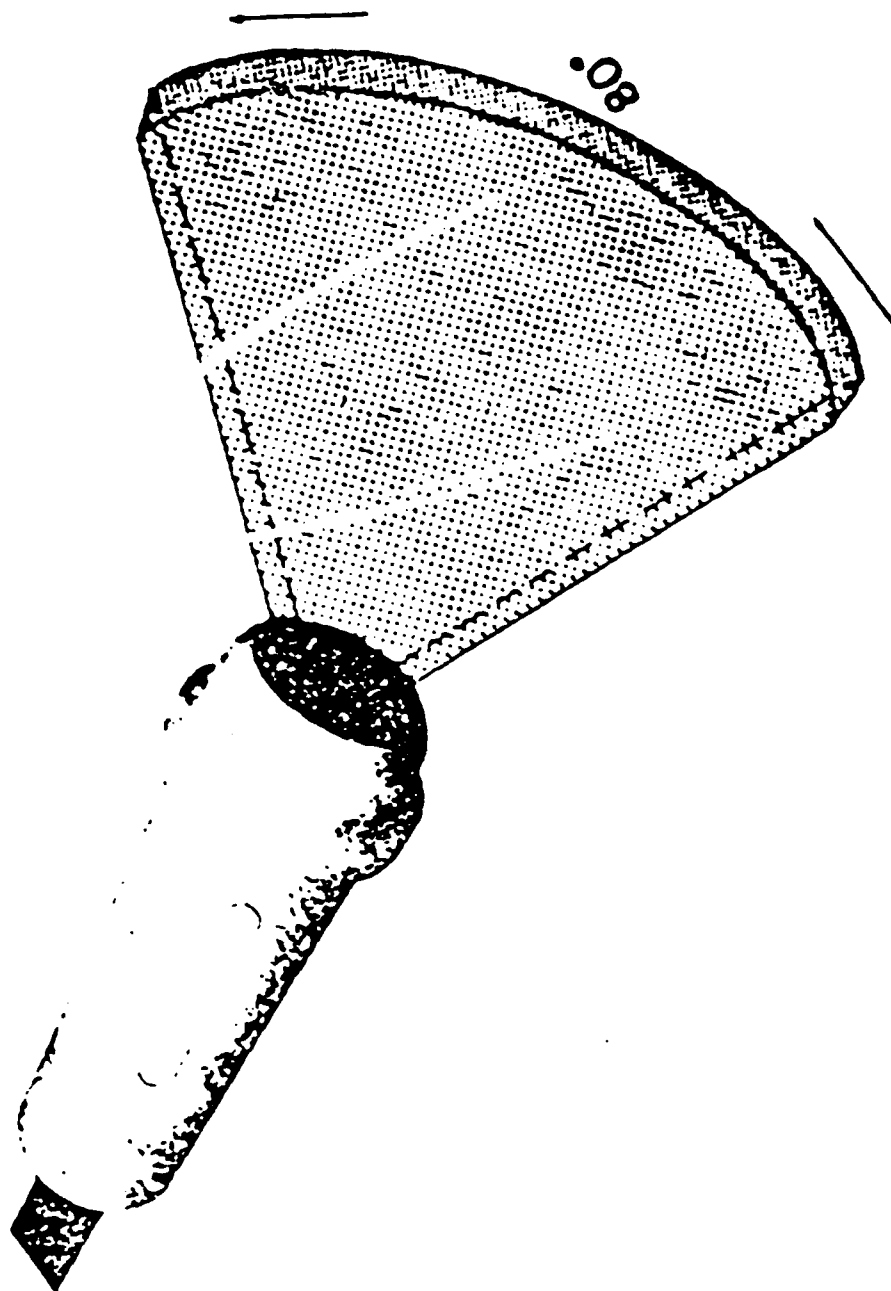
80.°

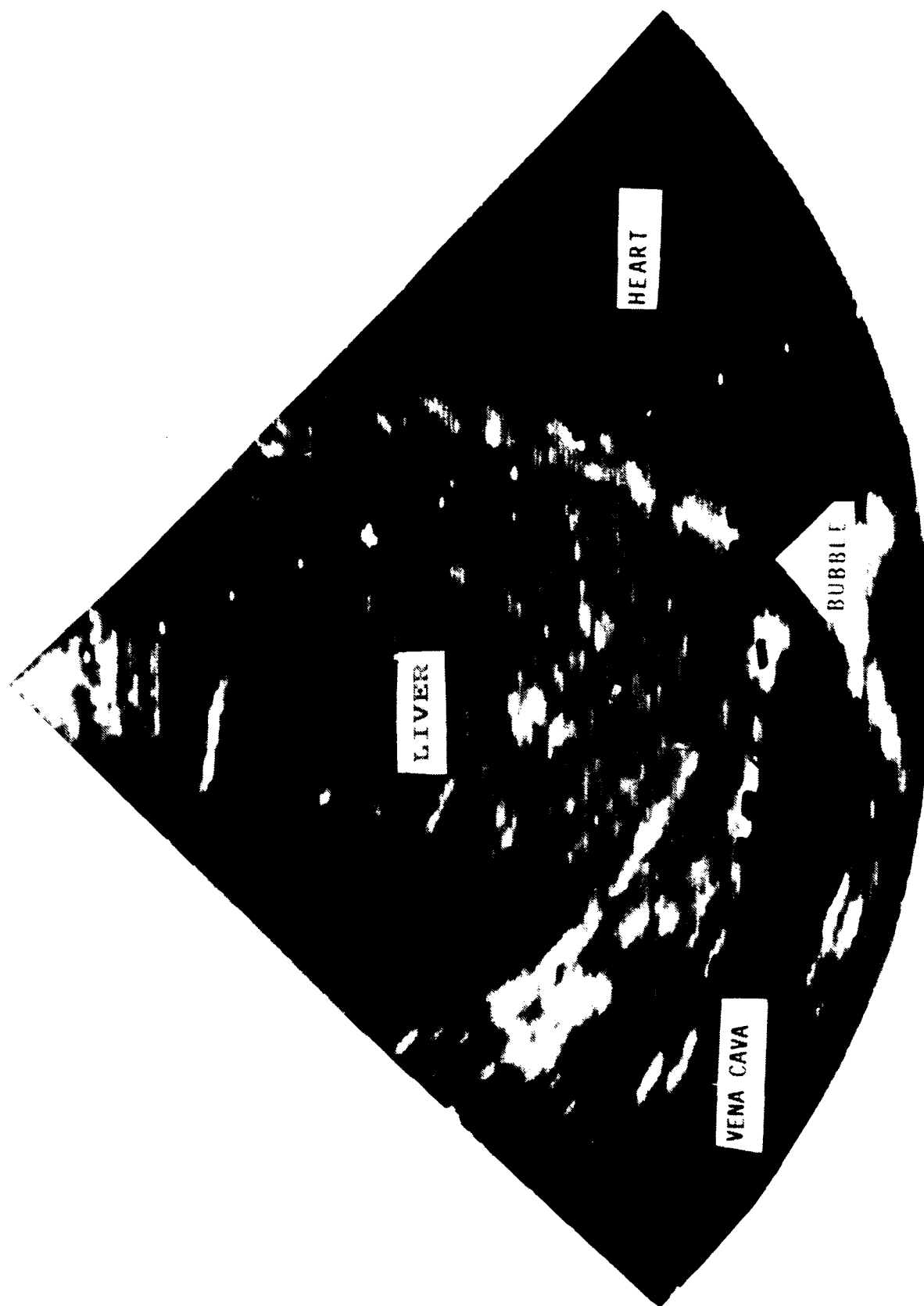Figure 2. The probe for the imaging system.

ECHO IMAGING SECTOR SCAN

Figure 3. An example of the screen of the ECHO imaging system showing a view of the heart and vena cava through the liver.

HEART

LIVER

BUBBLE

VENA CAVA

chamber monitored the subjects using the Sonos 1000. The details of the technique are described in the literature (4,5). Briefly, joint flexion is used to dislodge VGE from a particular joint. Consequently, they can be imaged as they flow through the heart. By flexing each joint sequentially, it is possible to determine which limb is the source of the VGE. The transducer of the Sonos 1000 monitoring system inside the chamber was connected by cable to the rest of the system located outside the chamber. To correctly position the transducer over the subject's heart, the technician relied on the 2-D scan on a TV monitor outside the chamber next to a window. The subject remained at altitude until he either developed DCS or completed a 4 h exposure. If VGE developed during the exposure, the subject's IVC was monitored to determine if the VGE seen in the heart could also be seen flowing in this vessel. Monitoring was done with the subject lying supine with his knees flexed. The investigator positioned the probe on the skin in the midline of the abdomen just below the rib cage. The aim of the transducer was adjusted until the IVC could be imaged as in Figure 3. Then the subject, holding his breath so that the IVC would dilate, was told to flex the joint which had generated VGE. The resulting sector scan was recorded on tape.

It will be seen in the results section that the vast majority of VGE travel in the interior of the IVC and many are big enough to be imaged by the Sonos 1000. The sizing techniques have been developed based on this observation. It is necessary to use in-vitro techniques to understand the size relationship between bubble images and the actual bubbles. The first techniques to be discussed are those used in relative rather than absolute bubble sizing. Figure 4 a-c, discussed in detail in the results section, can be used here to illustrate some of the factors to consider. Figure 4b shows several bubble images indicated by arrows and labeled "b." One bubble image is considerably bigger and brighter than the others. It is reasonable to assume that this represents the biggest bubble. The first set of in-vitro experiments test this hypothesis.

In Vitro Studies

Relative Bubble Size

A jar with optically and ultrasonically transparent walls was filled with water and shaken. Bubbles in the fluid were observed with a light beam and magnifier. It was determined that relatively big bubbles float relatively fast. Then, the fluid was observed ultrasonically with the probe against the jar so that the emitted ultrasonic beam (see Figure 2) was vertical. The flotation rate of the bright bubble images was compared to that of the dim bubble images.
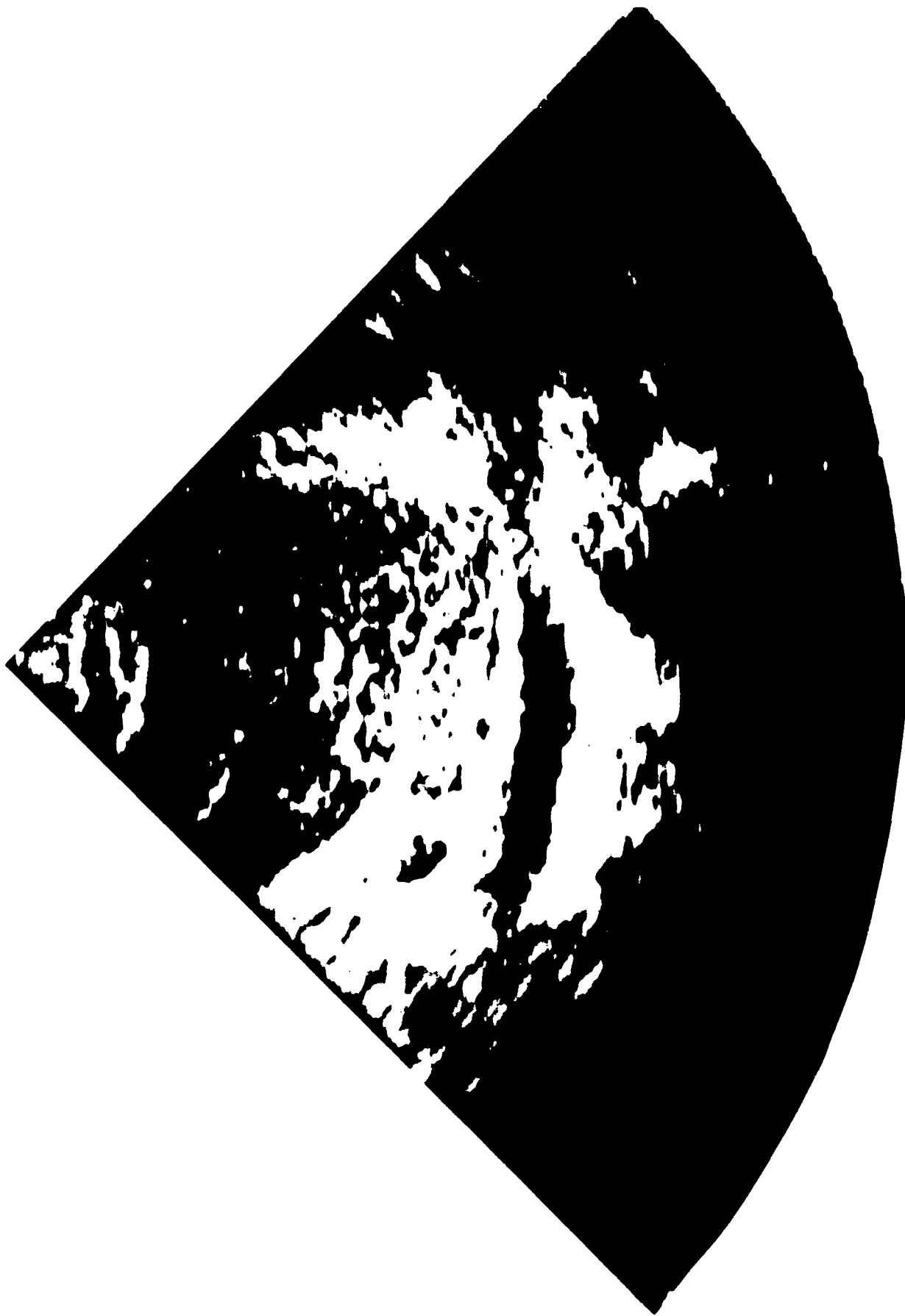
6

Figure 4a-c. Consecutive pictures of bubbles entering the inferior vena cave of a decompressed subject.
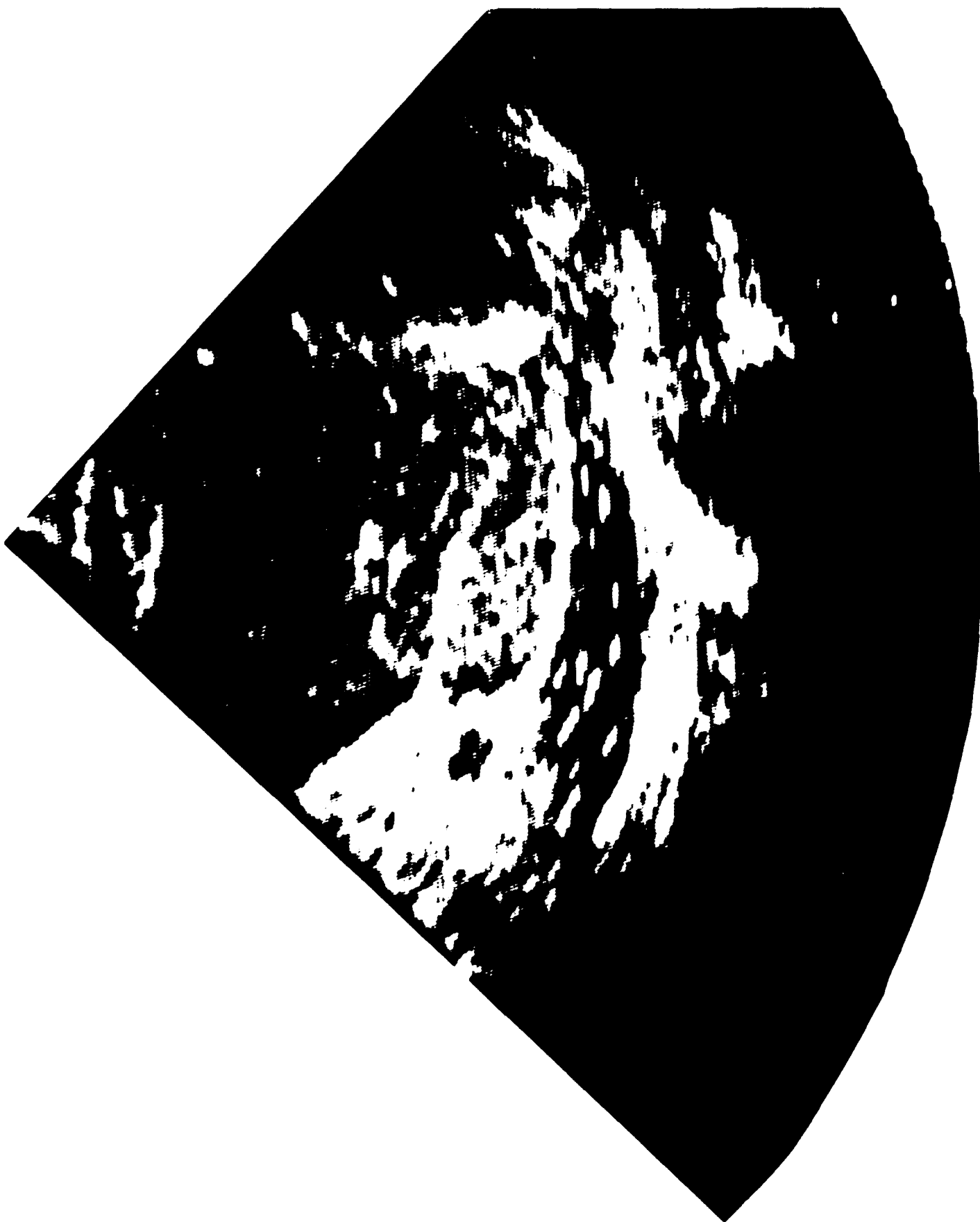
Fig. 4b

8

Fig. 4c

9

Absolute Bubble Sizing

The remaining in-vitro experiments were designed for absolute bubble sizing. The first step in absolute bubble sizing was to determine the size of the smallest bubble which the Sonos 1000 could detect. The first consideration is the probe-to-target distance, D. It is likely that this "just detectable bubble size" varies with D. For these experiments, D was chosen as 8-10 cm, the distance of the IVC from the probe in our subjects. Another consideration is the nature of the intervening tissue. As can be seen in Figure 3, this tissue is almost entirely liver tissue in the subjects. Therefore, it was necessary to use liver tissue in the in-vitro model. The next consideration is how to generate bubbles of a range of known sizes which might be expected in the IVC. This could be a formidable task because many bubbles whose size differed only slightly would be needed. Fortunately, it is possible to create bubbles covering a wide range of sizes simply by shaking a partially filled container of water. Their size can be determined from their behavior, i.e., flotation rate and survival time. Both of these characteristics can be measured optically as well as ultrasonically. For example, it was found microscopically that bubbles less than 40 μM in diameter float very slowly. In fact, their motion is determined primarily by eddy currents in the fluid. Likewise, it was found that bubbles approximately 25 μM in diameter collapse in seconds while bubbles larger than 50 μM persist for minutes and 100-μM bubbles last for hours. An important exception, that very small bubbles seem to be stable, will be discussed later in more detail. It is possible, therefore, to determine the size of a bubble whose image is on the Sonos 1000 screen simply by noting its survival time and flotation rate.

Lower Size Limit

The apparatus used to determine the smallest detectable bubble consisted of a 12-cm long piece of optically and ultrasonically transparent dialysis tubing 2.9-cm in diameter. It was fitted with corks at both ends. One cork was solid and the other had a hole bored through it so that the end of a syringe could be inserted into the cork. Water in the syringe could be injected into the tubing. The water used in these experiments had been filtered to remove any dirt greater than 0.2 μM in diameter. Water was drawn into the syringe, shaken with air, and then injected into the tubing. The tubing was placed horizontally so that bubbles in the fluid caused by shaking floated to the top side of the tubing. The tubing was observed under a microscope and the size of the bubbles determined using a standard technique in which the observer used one eye to look at the bubble through the microscope and the other eye to look at pictures of bubbles of various sizes on a sheet of paper. The object is to find the right bubble size on the paper and superimpose that picture over the bubbles seen with the other eye. The bubbles floating to the top side of the tubing were over

40 μM in diameter. Bubbles smaller than this float very slowly. The bubbles shrank and eventually collapsed. A chart of time to collapse vs. initial bubble size was created (Table 1). The same procedure was repeated using ultrasound by placing the tubing in a water bath whose depth was equal to the distance between the probe and the IVC in human subjects. As noted above, a thick slice of liver was inserted in the bath so that the ultrasonic beam would have to pass through this tissue just as liver tissue is in the path of ultrasonic beam in human subjects. Bubbles could be seen floating to the top of the tubing, but left behind were bubbles too small to float, yet big enough to be imaged. Their survival time was measured, and (from the previously created chart) their size was determined. After no bubble images could be seen ultrasonically, the tubing was placed under the microscope again and observed for microscopically visible bubbles.

Upper Size Limit

The last of the in-vitro techniques determined how small a bubble had to be to flow in the interior of the IVC. The apparatus used in this part of the experiment is shown in Figure 5. Figure 5 shows an analog of the IVC used in the third set of experiments. It consists of a piece of dialysis tubing, which is easily penetrated by ultrasound and is about the thickness of the IVC, suspended in a water bath. Connected to either end of the tubing are plastic tubes leading to gallon water reservoirs which could be raised or lowered one at a time to force water to flow through the tubing. On one of these sidearms, a T tube and a small piece of dialysis tubing were inserted so that bubbles could be introduced into the system and their size seen. These refinements are seen in Figure 5 at the extreme right. The depth of the water bath was about the depth of the IVC in subjects monitored ultrasonically. The velocity of flow could be adjusted to that seen in the subjects by adjusting the heights of the water reservoirs. The ultrasonic probe shown in Figure 2 was used to image bubbles in this mechanical analogue by positioning it just below the surface of the water above the dialysis tubing at which it was aimed.

The T tube has a side arm which is high enough so that water in the system does not run out the side arm when the reservoirs are in the resting position. A catheter can be run though the sidearm into the short segment of dialysis tubing inserted between the T tube and water bath which acts as a window. Bubbles of various sizes can be introduced through the catheter into the window and their size determined precisely by using the appropriate magnification and grids. The smallest bubble which can easily be introduced into the window through the catheter is 800 μM in diameter. Because solitary bubbles as small as 300 μM are needed, it was necessary to wait several hours until the bubble shrank to the desired size. (To hasten the process, water degassed by boiling was inserted into the window before the bubble.) Then the

11

Figure 5. A view of the apparatus to show at the extreme right a corked T tube through which a catheter can be passed to put bubbles in the short segment of dialysis tubing outside waterbath.

12

T tube sidearm was corked and the reservoirs moved to start flow. Turbulence develops in the window segment of the tubing so that the bubbles which at rest were on the wall now become dislodged and distributed throughout the fluid as it enters the tubing in the water bath.

In summary, two methods were used to measure absolute bubble size, one to determine the size of the smallest bubbles which could be imaged by the Sonos 1000 and the other to determine how big bubbles flow in the IVC. It will be seen that the flow characteristics of these relatively big bubbles sets an upper limit on the size of bubbles which flow in the interior of the IVC.

RESULTS

Instrumentation

An example of how the Sonos was used in subjects is shown in Figures 4a-c. VGE images which developed at altitude presisted and were recorded at ground level. Figure 4a was taken from the subject in a resting state where the vena cava is small. As in Figure 3, the IVC is represented by the 1-cm thick black band running horizontally about 10 cm from the probe. It empties into the heart, shown at the extreme right. In Figure 4b, the IVC is shown dilated as the subject holds his breath. Bubble images can be seen in the vessel, indicated by arrows. One of the images is quite large. It is located in the center of the vessel. Several small VGE images can be seen upstream near the vessel walls. Figure 4c shows a large number of VGE in the IVC. It is from images such as these that bubble sizing was done. Note that the images are not round like the bubbles they represent possibly due to the motion of the bubbles.

In Vitro

Relative Sizing

The first in-vitro study, as described in the Methods section, was designed to study relative bubble sizing. It tests the hypothesis that relatively large bubbles produce relatively bright images. For example, in Figure 4b one bubble image is much bigger and brighter than the others. Does this mean that the corresponding bubble is bigger? To answer this question, a bottle with ultrasonically transparent walls was filled with water and shaken to create bubbles of various sizes. It was viewed ultrasonically and optically (with a magnifier and side lighting). Various sized bubbles up to 200 μM in diameter were created. Ultrasonically, the bubbles appeared as in Figure 6. In Figure 6, bubble images of varying intensity can be seen between the apex

13

at the left and the image of the container wall which appears as a solid white vertical band toward the right side of the figure. These bubbles floated to the surface of the fluid at a rate which varied their size. The relatively large bubbles floated faster than small ones and the relatively bright images move faster than the small faint ones. This relationship demonstrated that, at least for slow moving bubbles, relatively large bubbles produce relatively large and bright images. For bubbles moving as fast as those in the IVC, the bubble images appear smeared, as already noted. Therefore, if two bubbles whose sizes are to be compared are moving rapidly at different velocities (both direction and speed), their images may be smeared differently so they cannot be compared. Fortunately, there are times during the cardiac cycle when flow near the heart is slow enough so this is not a problem. Although it has not been actually seen in these experiments, theoretically there is one other complication. It involves the position of the bubbles relative to the ultrasonic beam. Recall in Figure 1b that the ultrasonic beam is fan shaped, but it has depth. It is appropriate to talk about a front, back and middle of this beam. Bubbles in the middle of the beam are likely to be brighter than those in the front or back of the beam. For the IVC, bubble intensity is not a problem because the probe is positioned so that the IVC passes through the middle of the beam.

Lower Size Limit

The next part of the experiment was designed to determine the size of the smallest bubble which the Sonos 1000 could image. The bubbles formed by shaking water in a syringe were injected into a short piece of dialysis tubing which was placed on its side and observed under a microscope. Bubbles could be seen to float and come to rest immediately beneath the uppermost walls of the tubing. The size of these bubbles was measured by the technique described in the Methods section. Most bubbles were larger than 35 μM. If the plane of focus was changed from the tubing wall to the fluid inside the tubing, bubbles smaller than 35 μM could be seen suspended in the fluid, apparently too small to float. The time for bubbles, which had floated to the tubing walls, to shrink and disappear was measured and recorded in Table 1.
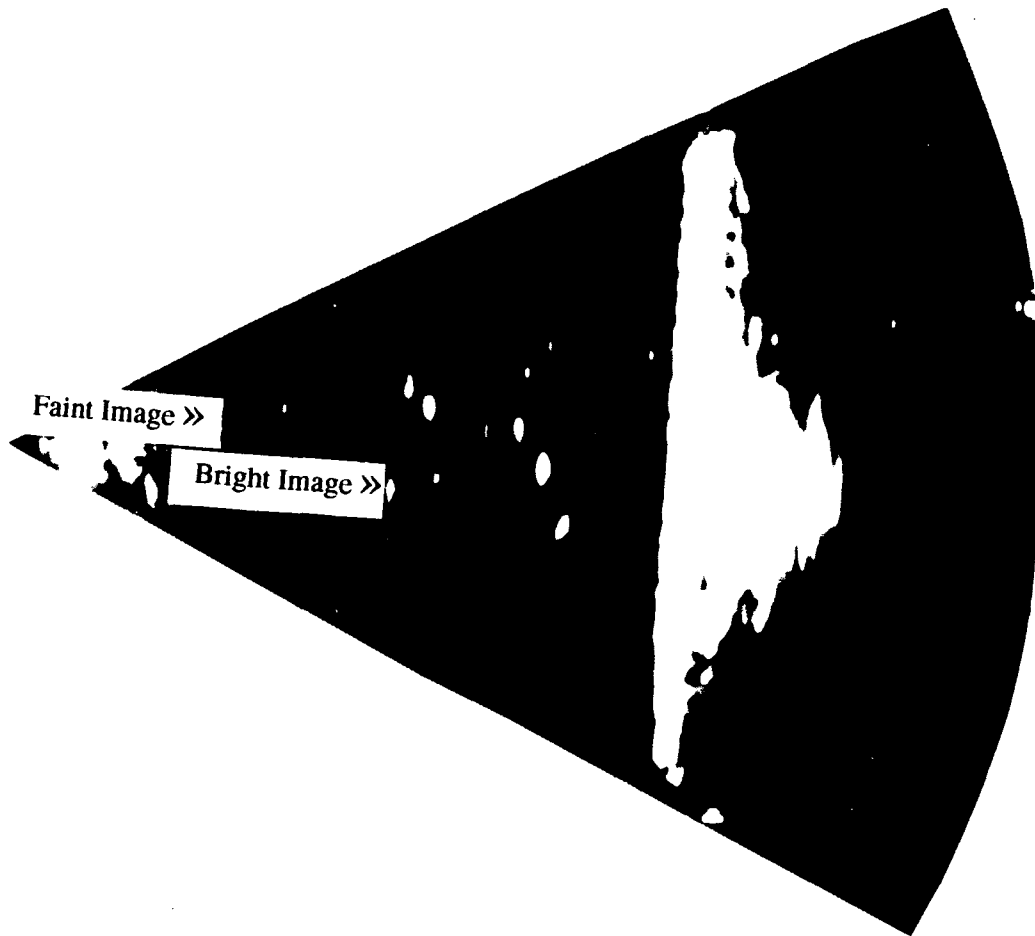
14

BUBBLE CLOUD

Faint Image »

Bright Image »

Figure 6. Images of various sized bubbles.

Table 1.   BUBBLE SIZE AND SURVIVAL TIME

| Initial Bubble Diameter	Time to Disappearance
100 μM	over 7 minutes
50 μM	1-7 minutes
25 μM	less than 60 seconds

15

Note that the values in the chart are specific for the conditions of this experiment. They depend, for example, on the degree of gas saturation of the water used in the tubing. The same saturation was used throughout the experiment. The chart above refers mostly to bubbles large enough to float. Note that values are also given for bubbles as small as 25 μM. These values were obtained by allowing larger bubbles to shrink until the desired initial diameter was obtained. Then the time to their disappearance was recorded. From the microscopic studies, then, two bubble characteristics have been learned. First, the motion of bubbles less than 30-40 μM in diameter is determined by eddy currents in the fluid rather than flotation. Second, the survival time of small bubbles depends on their initial size as shown in Table 1.

This information was used to determine the size of the smallest detectable bubble as follows. The same procedure for generating bubbles was followed. However, this time the bubbles in the tubing were observed ultrasonically by placing the tubing in a water bath which mimicked conditions in a human subject. Namely, the distance between the probe and target was about 8 cm and some of the intervening space was occupied by liver tissue. The top of Figure 7 shows the ultrasonic image of the dialysis tubing which had just been filled with bubble laden water. This tubing extends vertically between 6 and 8 cm from the probe. It was observed that, in the first few seconds, many bubbles floated toward the top of the fluid column. The sector scan at the bottom of Figure 7, which shows the same tubing a few seconds later, demonstrates that a sharp demarcation develops between the bubble-laden fluid at the top of the tubing and the almost bubble free-fluid at the bottom. Close inspection shows, however, that there are a few faint bubble images in the bottom. These are images of bubbles which were too small to float at an appreciable rate. From the microscopic observations, bubbles too small to float are less than 30-40 μM. Therefore the remaining bubbles imaged ultrasonically were less than 30-40 μM. They gradually decreased in size and disappeared over a 50-sec interval. From Table 1, this observation confirms that the bubbles must be smaller than 30-40 μM because larger bubbles would survive for long periods of time. The tubing was then observed microscopically and bubbles of all sizes up to 5-10 μM could still be seen. As expected, the ultrasonic imaging system cannot image these bubbles 10 μM or less. In summary, 40 μM bubbles were ultrasonically imaged but 30 μM bubbles were not.

Upper Size Limit

The variety of VGE image size and brightness seen in some recordings from human subjects suggests that there is considerable variability in VGE size. As just discussed, the smallest bubbles are 30-40 μM in diameter. In the last part of the in-vitro experiments, the largest VGE in the interior of the IVC was determined using the apparatus in Figure 5, in which a 300 μM bubble was placed by catheter in the window as described in the

16

ULTRASONIC IMAGES
OF
BUBBLES IN DIALYSIS TUBING

Bubbles in Tubing »

Bubbles in Tubing »

Bubbles in Tubing »

Bubbles in Tubing »
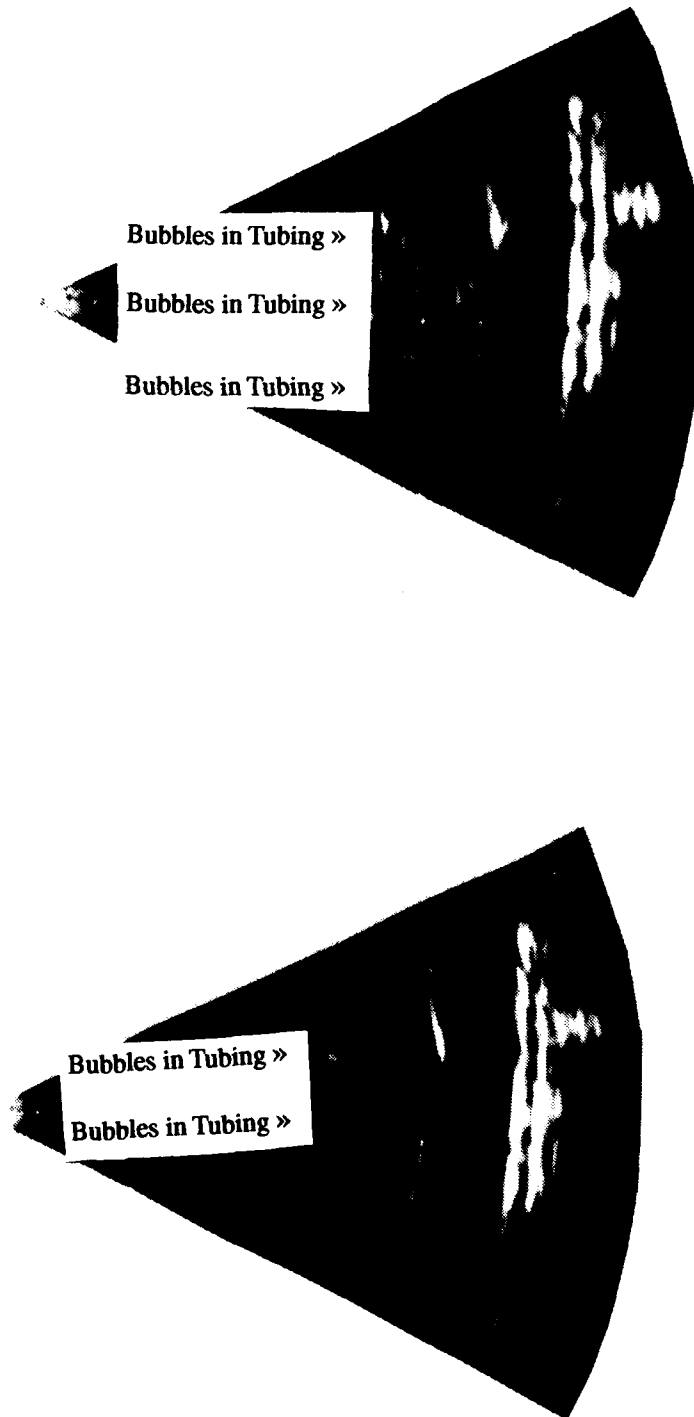
Bubbles in Tubing »

Figure 7. Dialysis tubing filled with bubbles in water bath 6-8 cm from probe.

Methods section. When flow was started, this bubble, after it was dislodged from the wall by the turbulence in the window segment, entered the long submerged tubing where flow was laminar. Instead of staying in its streamline, it floated up to the top of the tube in a short distance and then rolled along the top of the vessel. Figure 8a shows two bubbles entering the model of the IVC which runs laterally about 10-12 cm from the probe. One bubble, about 10.5 cm from the probe, was 300 μM as measured in the window, and one about 11 cm from the probe was 100 μM. Figures 8b and 8c, taken a few milliseconds later, show how the smaller bubble stays in its streamline, while the larger bubble rises to the top of the vessel. It was concluded that if a bubble is big enough, it will roll along the top of the vessel rather than stay in the streamlines. For water, this critical size is about 300 μM. For blood flowing in the IVC, the size may be a little larger due to blood viscosity. An example of a VGE which rolled along the top of the IVC is shown in Figure 9a. The arrow points to this bubble. In the next frame as shown in Figure 9b the bubble has moved slightly downstream. Note that the bubble image is brighter than images from the bubbles inside the IVC. This different brightness suggests that the bubble rolling along the top of the vessel is relatively large. One might conclude that the vast majority of VGE which flow inside the IVC are less than 300 μM in diameter because very few are large enough to roll along the top of the vessel.

DISCUSSION

Several comments regarding the sizing technique need to be made. Relative bubble sizing can be very useful and is free from many of the problems associated with absolute sizing. So long as the bubbles to be compared are in close proximity, then the probe-to-target distance, intervening tissue ultrasonic impedance, control settings and bubble position relative to the ultrasonic field are the same for each bubble. By relative sizing, it has been shown that the bubbles in the IVC of altitude-exposed subjects can cover a wide range of sizes. Sometimes, however, the bubbles are remarkably similar in size, a size expected for bubbles originating in venules rather than capillaries.

The discussion of absolute sizing began with the lower size limit of bubbles seen ultrasonically in the IVC. Methods used to determine the smallest sized bubbles which the echo imaging system could detect, based on in-vitro studies, were done first. The in-vitro conditions were set up to mimic those found in the IVC. The most direct approach would be to manufacture microbubbles or glass spheres of progressively smaller sizes and find the smallest ones which could be imaged. This difficult, tedious process was avoided. Figure 7 summarizes the fortuitous finding that bubbles too small to float can still be displayed by the ultrasonic system even though they are too small to see, except possibly as dots, without a microscope. Therefore, imaging systems are actually able to image bubbles in the microscopic range, a truly remarkable
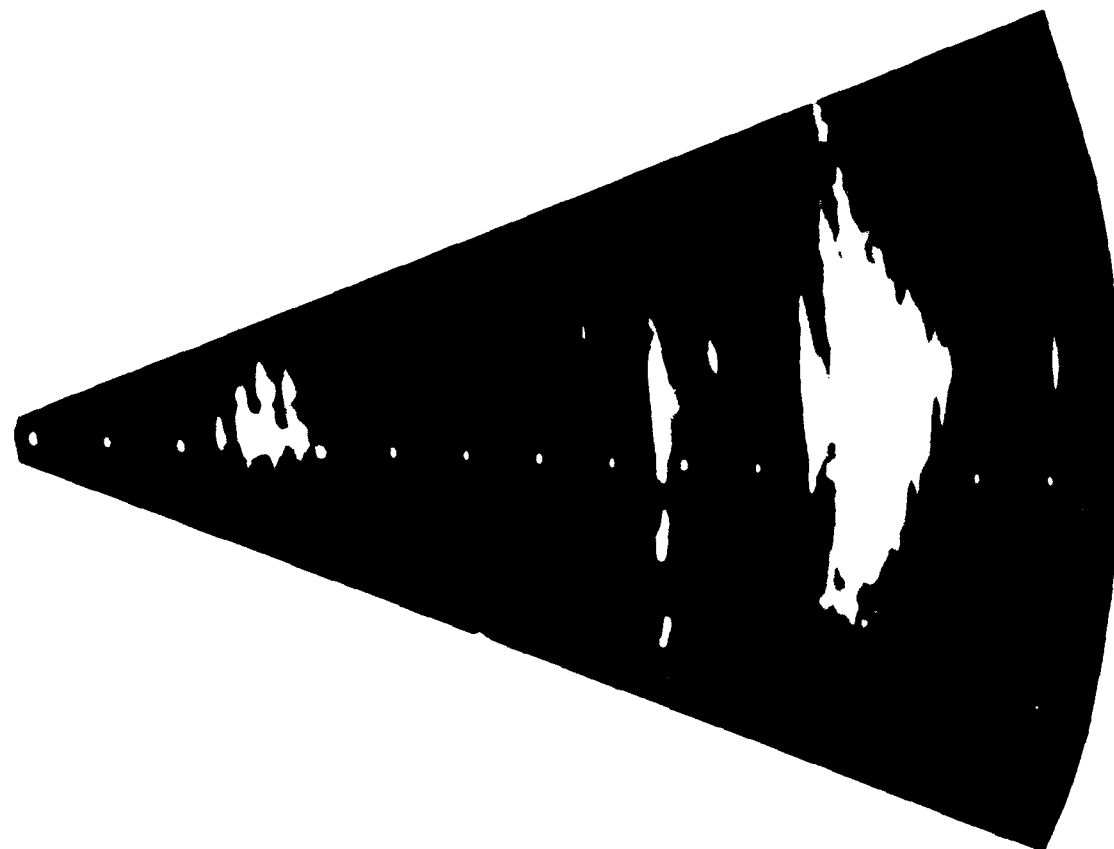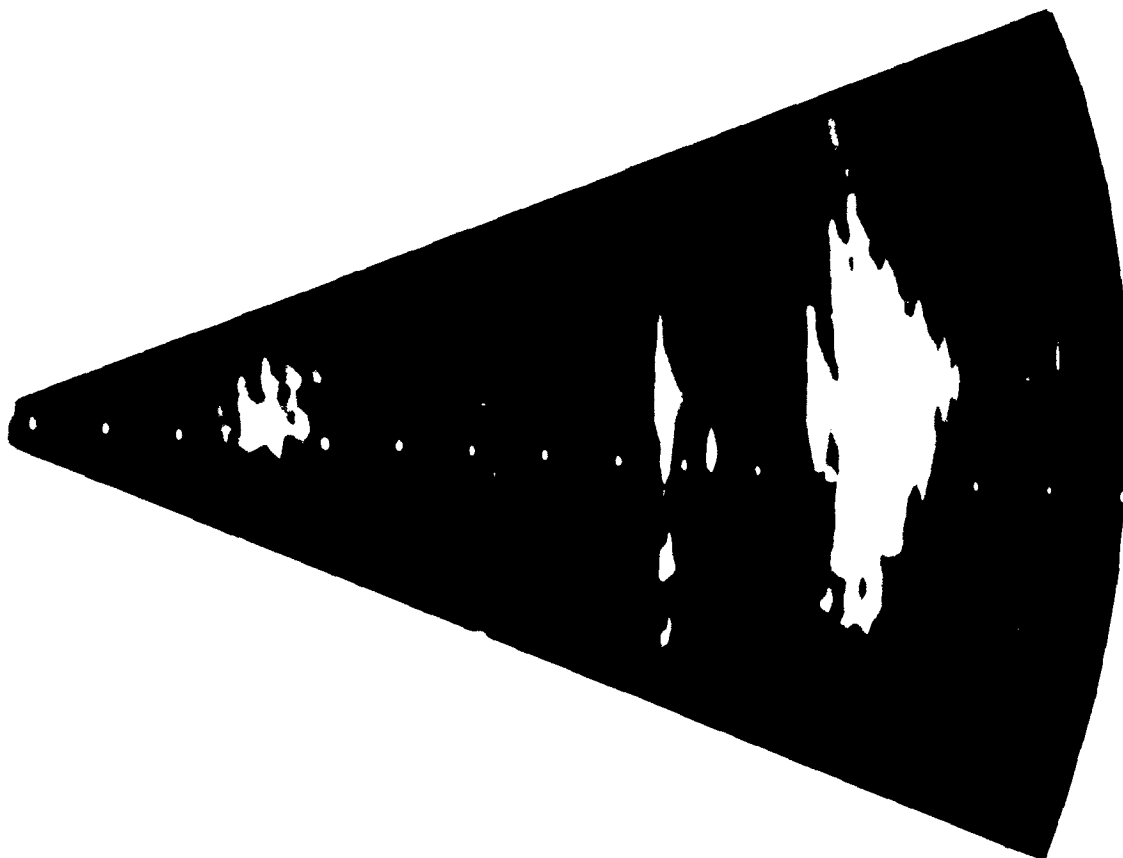
18

Fig. 8b

Fig. 8a

Figure 8a-d. Consecutive pictures of a large and small bubble moving down the tubing of the mechanical analog. Note that the big bubble rises to the top of the tubing.
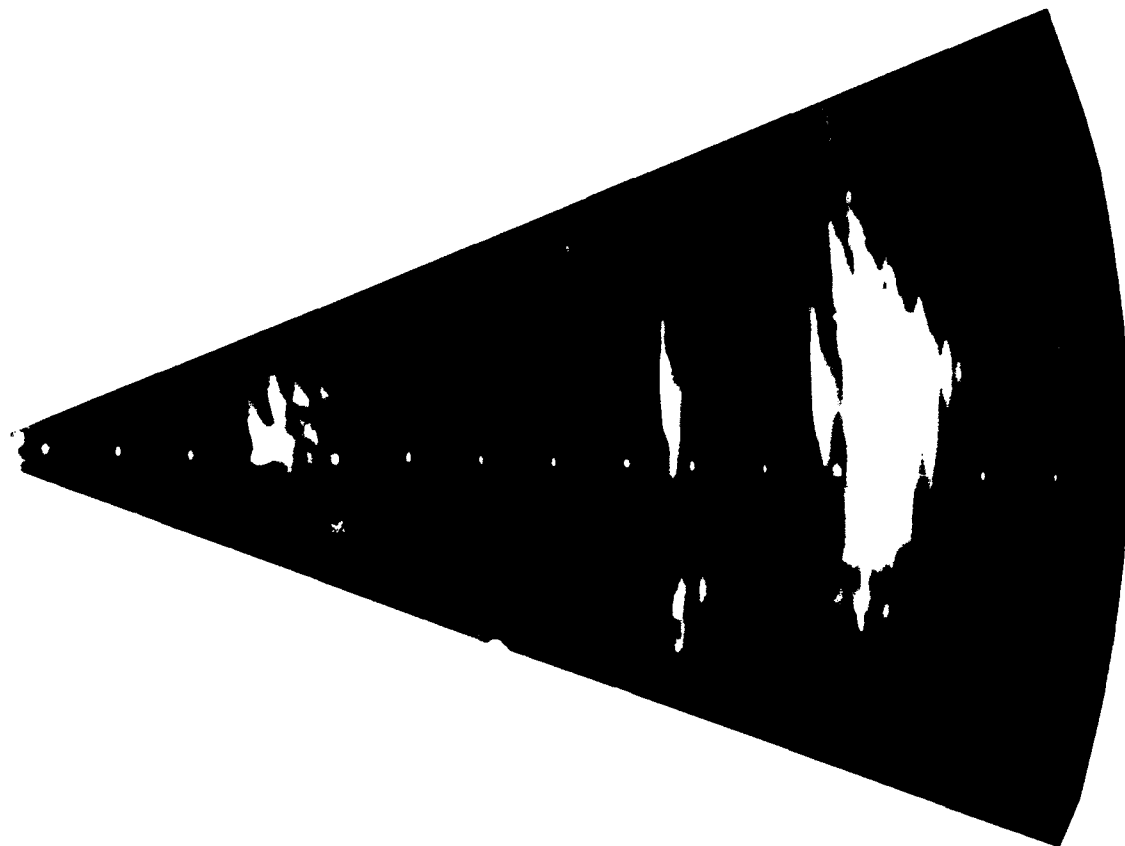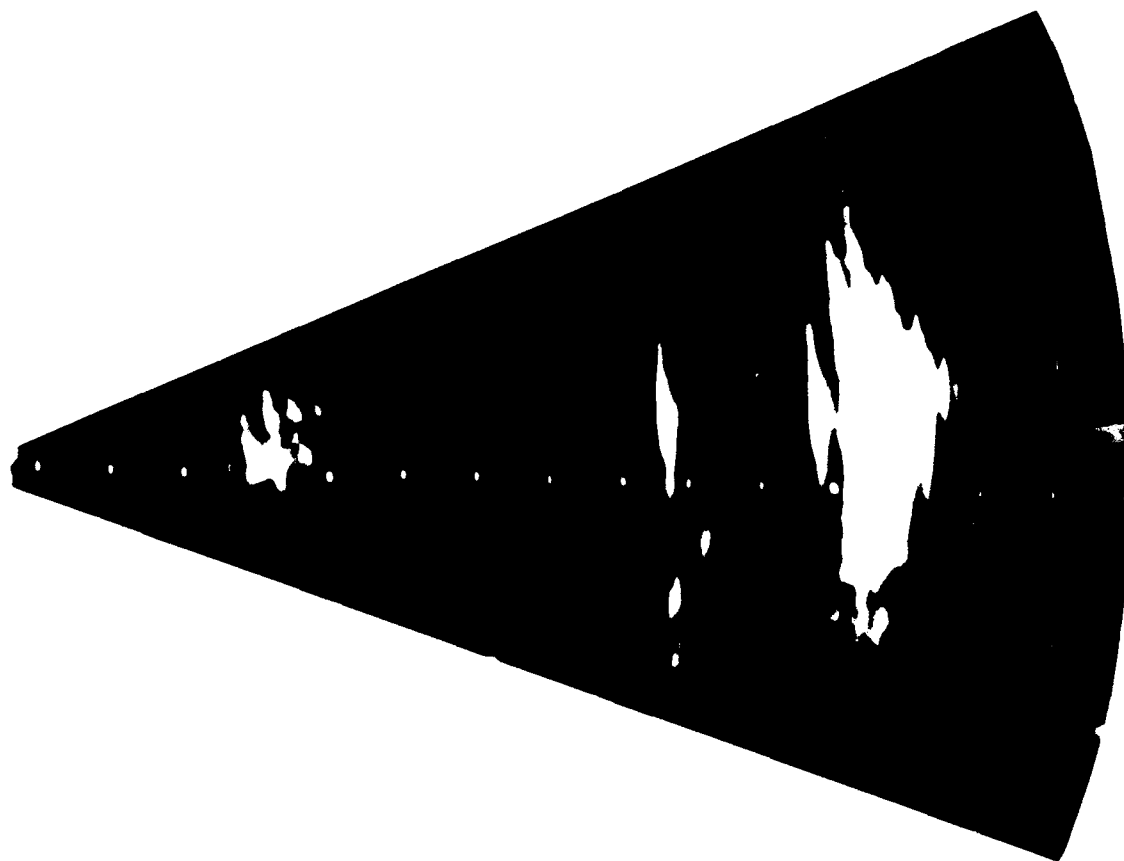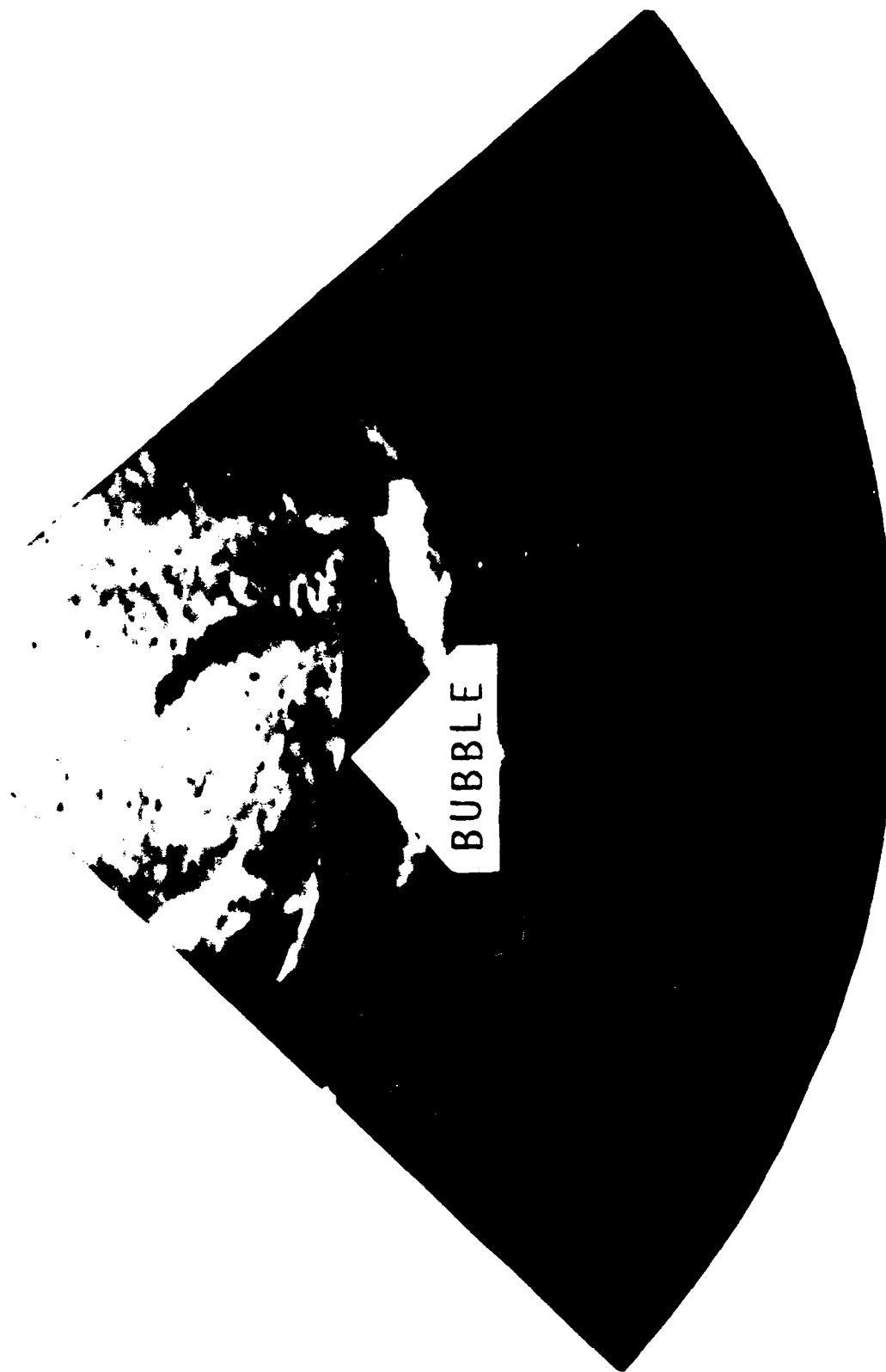
19

Fig. 8d

Fig. 8c

Figure 9a,b. Two successive frames in which a big bubble can be seen at the top of the IVC.

BUBBLE

Fig. 9b

22

capability. Note in Figure 7 how faint the small non-floating bubble images appear. Even though they can be imaged, 30-40 μM bubbles are not easily seen. Although a few of these small VGE can be seen occassionally in the IVC, most of the VGE are bigger than this. The data of this experiment suggest that, if one were to graph the number of bubbles vs the size of bubbles in the IVC, the largest number of bubbles would be well within the detectable size range of the Sonos. In the Methods section and again in the Results section, it was noted that very small bubbles seem to be stable and do not collapse as expected by theory or observation of bigger bubbles. These small, stable microbubbles are too small to be imaged by the Sonos 1000. They could be present but undetected in the IVC of decompressed subjects. A discussion of this phenomenon is given in the literature (3, p. 68).

The final part of the sizing technique, which uses the IVC analog for detecting the upper size limit of VGE, is the weakest part of the technique because blood, due to its opacity, had to be replaced by water. The same phenomenon observed in decompressed subjects, however, was duplicated in the model. Namely, bubbles big enough to roll along the top of the vessel were created. Their size was measured. Bubbles or VGE which stay in the interior of the IVC must be smaller than these bubbles, which therefore indicate the upper size limit.

Several reasons why DCS bubble size is of interest were listed in the Introduction. One of these reasons was that bubble size may help establish where bubbles are arising. When a subject flexes a joint at altitude and bubbles appear shortly thereafter in the IVC, it seems reasonable to assume that the bubbles arise from tissues in the flexed joint. Bubbles as big as 300 μM were found in some subjects. They must be coming from venules rather than from capillaries. When the bubble cloud dislodged by flexion consists of heterogenous sized bubbles, as was the case in some of our subjects (see Figure 4), bubbles must arise from a variety of different sized vessels. In some subjects, homogenous bubble size indicated that all bubbles arose from the same sized vessels. Another reason for interest in bubble size relates to the destiny of bubbles. Since many bubbles are bigger than capillary size, vascular occlusion in the lung must occur. However, the proximity of pulmonary vasculature to alveoli makes it possible for gas to diffuse out of the bubbles and through the vessel walls rapidly. The lung acts as an effective filter and sink for bubbles. A final reason for bubble sizing involves the phenomenon of "silent bubbles", a phenomenon which undermines the value of ultrasonic monitoring of decompressed subjects. A subject who develops bubbles but no symptoms, i.e., silent bubbles, is a false positive as far as the ultrasonic monitoring system is concerned and indicated treatment would be inappropriate. Silent bubbles are more frequent at low altitudes where bubbles are relatively small. Therefore, it is reasonable to suppose that silent bubbles are too small to cause symptoms. Until now, it has not been possible to prove this hypothesis because bubble size could not be measured.

Interest in ultrasonic bubble sizing may not be restricted to decompression sickness. Because bubbles are excellent contrast material for ultrasonic systems, they are used frequently in clinical applications of ultrasound, such as in the detection of patent ductus arteriosis. Future techniques will almost certainly use microbubbles in the study of such things as myocardial blood flow and tumor structure.

REFERENCES

1. Chapelon JY, Shankar PM, Newhouse VL. Ultrasonic measurement of bubble cloud size profiles. J. Acoust. Soc. Amer. 1985; 78:196-201.

2. Dixon GA, Adams JD, Harvey WT. Decompression sickness and intravenous bubble formation using a 7.8 psia simulated pressure-suit environment. Aviat. Space and Environ. Med. 1986; 57:223-8.

3. Hills, BA Decompression sickness. New York: John Wiley, 1977:49-97.

4. Olson, R.M., A.A, Pilmanis and T.E. Scoggins. Use of Echo Imaging in Decompression Model Development. Abstract Avait. Space and Environ. Med, May 63 (5) pp386, 1992.

5. Olson RM, Krutz RW Jr, Dixon GA, and Smead KW. An evaluation of precordial ultrasonic monitoring to avoid bends at altitude. Aviat. Space and Environ. Med. 1988; 59:635-9.

6. Shankar PM, Chapelon JY, Newhouse VL. Fluid pressure measurement using bubbles isonified by two frequencies. Ultrasonics 1986; 24:333-6.

7. Spencer MP, Clarke HF. Precordial monitoring of pulmonary gas embolism and decompression bubbles. Aerospace Med. 1972; 43:762-7.

8. Van Liew, H.D. and M.P. Hlastala. Influence of bubble size and blood perfusion on absorption of gas bubbles in tissues. Respiratory Physiology, 7, 111-121, 1969.